



## RESEARCH LETTER

10.1002/2017GL076667

## Key Points:

- Anthropogenic aerosols induce an overall reduction in Asian monsoon rainfall and circulation
- Fast adjustments dominate aerosol-induced monsoon changes over land north of 20 degree N, largely driven by aerosol-cloud interactions
- Sea surface temperature feedbacks (slow response) cause substantial changes in the monsoon meridional circulation over the oceanic regions

## Supporting Information:

- Supporting Information S1

## Correspondence to:

X. Li,  
xqli@ldeo.columbia.edu

## Citation:

Li, X., Ting, M., & Lee, D. E. (2018). Fast adjustments of the Asian summer monsoon to anthropogenic aerosols. *Geophysical Research Letters*, 45. <https://doi.org/10.1002/2017GL076667>

Received 12 DEC 2017

Accepted 27 DEC 2017

Accepted article online 3 JAN 2018

©2018. The Authors.

This is an open access article under the terms of the Creative Commons Attribution-NonCommercial-NoDerivs License, which permits use and distribution in any medium, provided the original work is properly cited, the use is non-commercial and no modifications or adaptations are made.

## Fast Adjustments of the Asian Summer Monsoon to Anthropogenic Aerosols

Xiaoqiong Li<sup>1,2</sup> , Mingfang Ting<sup>2</sup> , and Dong Eun Lee<sup>2</sup> 

<sup>1</sup>Department of Earth and Environmental Sciences, Columbia University, New York, NY, USA, <sup>2</sup>Lamont-Doherty Earth Observatory, Columbia University, Palisades, NY, USA

**Abstract** Anthropogenic aerosols are a major factor contributing to human-induced climate change, particularly over the densely populated Asian monsoon region. Understanding the physical processes controlling the aerosol-induced changes in monsoon rainfall is essential for reducing the uncertainties in the future projections of the hydrological cycle. Here we use multiple coupled and atmospheric general circulation models to explore the physical mechanisms for the aerosol-driven monsoon changes on different time scales. We show that anthropogenic aerosols induce an overall reduction in monsoon rainfall and circulation, which can be largely explained by the fast adjustments over land north of 20°N. This fast response occurs before changes in sea surface temperature (SST), largely driven by aerosol-cloud interactions. However, aerosol-induced SST feedbacks (slow response) cause substantial changes in the monsoon meridional circulation over the oceanic regions. Both the land-ocean asymmetry and meridional temperature gradient are key factors in determining the overall monsoon circulation response.

### 1. Introduction

Over the past few years, “Asian smog” has become one of the most pressing environmental threats around the world, featuring unprecedentedly high pollution levels and severe impacts onto the world’s most densely populated region. According to a study conducted by the Global Burden of Disease from Major Air Pollution Sources (GBD MAPS) Working Group, ambient fine particulate matter ( $PM_{2.5}$ ) is a major contributor to mortality and disease burden in China, with an estimated contribution of 916,000 deaths in 2013, among which 40% is caused by coal combustion (GBD MAPS Working Group, 2016). Apart from the direct health impacts, air pollution has been shown to affect meteorological conditions, as well as long-term climate variations (Boucher et al., 2013; Gong et al., 2007). Aerosols can affect global and regional climate by altering the radiation budget and interacting with clouds through microphysical processes, thereby causing subsequent changes in surface temperature as well as the hydrological cycle (Allen & Ingram, 2002; Levy et al., 2013; Li et al., 2016; Ming et al., 2010).

The most populated regions of the Asian continent are characterized by a distinct monsoonal climate, spanning from the Indian subcontinent to the extratropics of eastern Asia. The summer monsoon brings over 80% of the annual rainfall in these regions, essential for local economy, agriculture, ecosystems, and human health (Hong & Kim, 2011; Piao et al., 2010). In addition, as a major part of the summertime overturning circulation in the Northern Hemisphere tropics, the Asian monsoon has profound remote influences on the global-scale climate (Lin & Wu, 2012; Rodwell & Hoskins, 1996). Previous studies have shown that the Asian summer monsoon has weakened during the twentieth century, with anthropogenic aerosols being a likely cause (Bollasina et al., 2011; Ganguly et al., 2012a; Li et al., 2015; Ramanathan et al., 2005; 2005). However, the exact trends and reasons remain unclear with large uncertainties in climate model simulations (Turner & Annamalai, 2012).

Despite prominent influence of natural variability (Kumar et al., 2006; Li & Ting, 2015), the Asian summer monsoon is predominantly affected by greenhouse gases (GHGs) and aerosols in the twentieth century (Singh, 2016; Turner & Annamalai, 2012). It has been shown that GHGs and aerosols have significant competing effects on monsoon rainfall change, with aerosols dominating the total drying trend during the twentieth century (Li et al., 2015). A number of studies have addressed the possible physical mechanisms of aerosol-induced tropical rainfall and monsoon changes (Ganguly et al., 2012a; Guo et al., 2013, 2015; Hwang et al., 2013; Lau et al., 2006). Unlike GHGs that induce a strong atmospheric moistening through an increase in sea surface

temperature (SST), aerosols affect monsoon rainfall largely through changes in atmospheric circulation (Li et al., 2015). Increased aerosols in the atmosphere could reduce the surface solar radiation (“dimming” effect) that reduces the local SST gradient in the Indian Ocean (Chung & Ramanathan, 2006; Ramanathan et al., 2005) and introduces a hemispheric energy imbalance caused by the spatial inhomogeneity of aerosol distributions (Bollasina et al., 2011), as well as increase atmospheric stability through direct and indirect effects (Lau & Kim, 2017), contributing to weakened monsoon circulation. Some other studies find that aerosols may enhance monsoon rainfall and circulation over the South China Sea and western Pacific (Jiang et al., 2013) or cause an earlier onset and enhanced June rainfall over India (Bollasina et al., 2013) due to absorbing aerosols such as black carbon (Lau et al., 2006), indicating high complexity and uncertainty associated with aerosol-monsoon interactions.

From an energetics perspective, the response of the climate system to an external forcing involves two components on different time scales: the fast response without the mediation of SST and the slow response due to SST feedbacks (Allen & Ingram, 2002; Andrews et al., 2009). The fast and slow components may lead to differing responses in the hydrological cycle, often studied using idealized atmospheric general circulation model (AGCM) experiments with prescribed SSTs (Hsieh et al., 2013; Richardson et al., 2016; Shaw & Voigt, 2015). A number of studies have shown that GHGs may cause compensating effects due to direct radiative forcing (fast response) and SST change (slow response) in atmospheric circulation, particularly over the Asian monsoon region, leading to large uncertainties and model spreads in coupled model simulations (Li & Ting, 2017; Shaw & Voigt, 2015). Also, for GHGs, some studies have emphasized the importance of the fast adjustments in explaining the total rainfall responses (Bony et al., 2013; Li & Ting, 2017). However, for anthropogenic aerosols, it has been shown that the slow response due to SST change may dominate the total monsoon rainfall and circulation changes over India (Ganguly et al., 2012b) and East Asia (Kim et al., 2016), while the fast adjustments due to sulfate aerosols contribute to a slightly intensified East Asian monsoon (Kim et al., 2016), both studies using a single AGCM. How much of the total monsoon response can be explained by the aerosol fast response without the mediation of SSTs? What is the role of SST feedbacks? These questions have not been fully explored for aerosol forcing.

Here we examine the Asian summer (June–August seasonal mean, JJA) monsoon response to anthropogenic aerosols on different time scales, with a focus on the fast adjustments independent of SST changes. We analyze the physical mechanisms of the total and fast responses and discuss the possible role of SST feedbacks. We address the question by using a suite of coupled general circulation models (CGCMs) in the Coupled Model Intercomparison Project—Phase 5 (CMIP5), and AGCMs with prescribed aerosol concentration and SSTs. Model simulations and analysis methodology are provided in section 2. We present the aerosol-induced total and fast monsoon rainfall responses in section 3 and analyze the thermodynamic and dynamic mechanisms in section 4. The main conclusions are summarized in section 5.

## 2. Methods

### 2.1. Model Simulations

To examine the effect of aerosol forcing, we used multiple model simulations including both CGCMs and AGCMs. For CGCMs, we used output from CMIP5 models (Taylor et al., 2012) under the historical aerosol-only scenario, with monthly data from 1861 to 2005. The total response is quantified using the climatological difference between 1981–2005 and 1861–1885. To examine the fast response, we used idealized AGCM simulations with prescribed SST and sea ice concentration that are part of the CMIP5 archive. The control simulation (called “sstclim” in the CMIP5 archive) uses fixed climatological SST and sea ice concentration from the preindustrial control simulation, and preindustrial anthropogenic aerosols. The forced experiment (“sstclimAerosol” in the CMIP5 archive) uses the same SST and sea ice as the control simulation but with year 2000 aerosols from the CMIP5 historical simulations. The 30 year climatological difference between the forced and control simulations quantifies the fast response, thus independent of SST changes.

The CGCM and AGCM monthly outputs are available for 13 and 11 models (multiple realizations available for some of the CGCMs) in the CMIP5 archive, respectively, however with only 5 models in common (Table S1 in the supporting information). The results using all available models and the subset using the five common models are largely robust (Figure S1). Here we show the results using the five common models using only the first realization for consistency purposes. All model outputs were interpolated to a  $2^\circ \times 2^\circ$  spatial resolution.

We further performed idealized AGCM experiments using the Community Earth System Model (CESM) version 1.2.0 with F-compset to examine the slow response due to aerosol-induced SST changes. F-compset consists of interactive atmosphere model (Community Atmosphere Model, CAM5) and land surface model (Community Land Model 4.0, CLM4) with prescribed SSTs and sea ice concentration. A detailed description of the model can be found in Neale et al. (2012). We use 1.9° latitude × 2.5° longitude horizontal resolution, 26 vertical levels, and the *cam4* physics package with prescribed gases (except for water vapor) and bulk aerosols. The control simulation (CTRL) is run with year 1850 aerosol concentration and 1951–2000 climatological SST and sea ice concentration from the Hadley Centre Sea Ice and Sea Surface Temperature data set (Rayner et al., 2003). The forced experiment (AEROSST) uses the same aerosol and sea ice concentration as the control experiment but adding an SST anomaly derived from the CMIP5 historical aerosol forcing only simulations to the observed climatological SST (Figure S8). The SST anomaly is the climatological difference between 1981–2005 and 1861–1885 using the multimodel mean (MMM) of the five common CMIP5 models listed in Table S1. All other gaseous species are fixed at preindustrial levels. Both experiments are run for 60 years (after an initial 1 year spin-up); the climatological difference between AEROSST and CTRL quantifies the slow response.

## 2.2. Moisture Budget Analysis

We analyze the atmospheric moisture budget to quantify the changes in the hydrological cycle. A detailed derivation and discussion of the possible errors can be found in Li and Ting (2017) and Seager and Henderson (2013). In steady state, the following balance can be expressed in pressure coordinates as

$$\bar{P} - \bar{E} = -\frac{1}{g\rho_w} \nabla \cdot \overline{\int_0^{p_s} \mathbf{u}q \, dp} \approx -\frac{1}{g\rho_w} \nabla \cdot \sum_{k=1}^K \overline{\mathbf{u}_k q_k \Delta p_k}, \quad (1)$$

where  $P$  is precipitation,  $E$  is evaporation,  $g$  is gravitational acceleration,  $\rho_w$  is the density of water,  $p$  is pressure and  $p_s$  surface pressure,  $\mathbf{u}$  is the horizontal wind vector,  $q$  is specific humidity,  $k$  is the vertical level with a total of  $K$  (here  $K = 10$ , from 1,000 hPa to 200 hPa), and  $\Delta p$  is the pressure thickness. Overbars represent monthly mean values.

We then separate the moisture flux convergence term into the mean moisture convergence (MC) and the submonthly transient eddies (TE):

$$\bar{P} - \bar{E} \approx -\frac{1}{g\rho_w} \nabla \cdot \sum_{k=1}^K \overline{\mathbf{u}_k \bar{q}_k \Delta p_k} - \frac{1}{g\rho_w} \nabla \cdot \sum_{k=1}^K \overline{\mathbf{u}'_k q'_k \Delta p_k}, \quad (2)$$

where primes denote departures from monthly means. Here we approximate the transient eddy component using the difference between  $P-E$  and the mean moisture convergence due to limited availability of daily data.

To quantify the forced response, we define

$$\overline{\overline{\delta(\cdot)}} = \overline{\overline{(\cdot)_F}} - \overline{\overline{(\cdot)_C}} \quad (3)$$

to represent the difference between the forced (subscript  $F$ ) and control (subscript  $C$ ) experiments, where the second overbar denotes the 30 year climatological mean. Then the change in the mean moisture convergence can be derived as follows:

$$\begin{aligned} \overline{\overline{\delta MC}} &= \left( -\frac{1}{g\rho_w} \nabla \cdot \overline{\overline{\sum_{k=1}^K \mathbf{u}_{k,F} \bar{q}_{k,F} \Delta p_{k,F}}} \right) - \left( -\frac{1}{g\rho_w} \nabla \cdot \overline{\overline{\sum_{k=1}^K \mathbf{u}_{k,C} \bar{q}_{k,C} \Delta p_{k,C}}} \right) \\ &\approx -\frac{1}{g\rho_w} \nabla \cdot \sum_{k=1}^K \overline{\overline{\mathbf{u}_{k,C} \delta \bar{q}_k \Delta p_k}} - \frac{1}{g\rho_w} \nabla \cdot \sum_{k=1}^K \overline{\overline{\delta \mathbf{u}_k \bar{q}_{k,C} \Delta p_k}} \\ &= \overline{\overline{\delta TH}} + \overline{\overline{\delta DY}}. \end{aligned} \quad (4)$$

Here for the thermodynamic component ( $\delta TH$ ), circulation ( $\mathbf{u}$ ) is fixed at the CTRL climatological value, thus representing changes due to specific humidity ( $q$ ); and for the dynamic component ( $\delta DY$ ), specific humidity ( $q$ ) is fixed at the CTRL climatological value, thus representing changes due to circulation ( $\mathbf{u}$ ). The quadratic term involving covariances of departures from climatological values of  $\mathbf{u}$  and  $q$  is small compared to  $\delta TH$  and  $\delta DY$  (Figure S5).

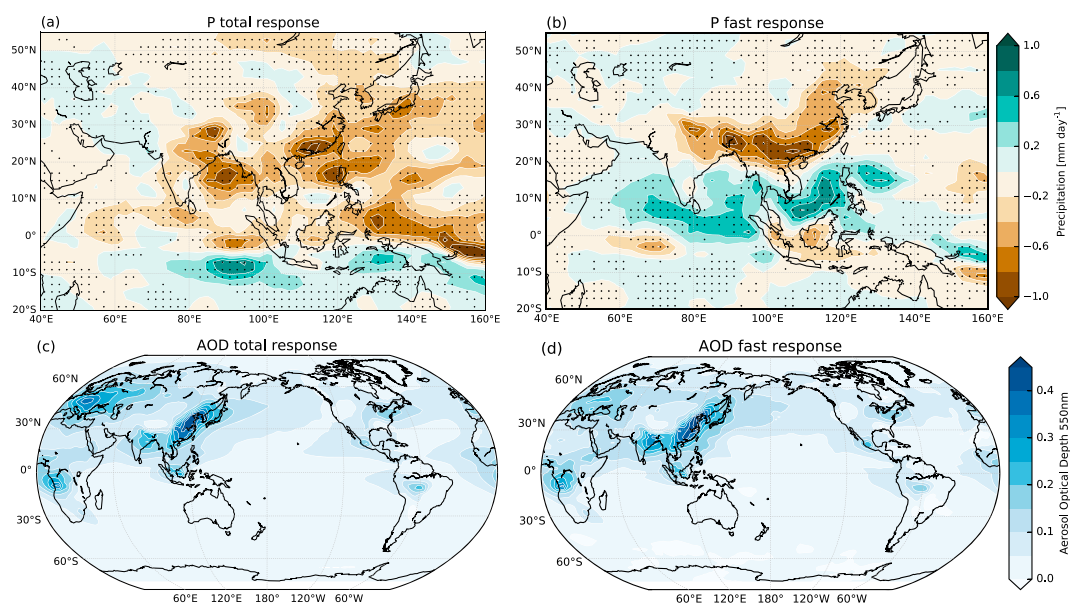


**Figure 1.** Precipitation response and the corresponding aerosol forcing. (a, c) Total response in CGCMs and (b, d) fast response in AGCMs of precipitation (Figures 1a and 1b) and 550 nm aerosol optical depth (AOD) (Figures 1c and 1d) to historical aerosol forcing using the five common models (AOD data are only available for three of the five models). In Figures 1a and 1b, stippling denotes four out of five models agree on the sign of change, units are  $\text{mm d}^{-1}$ .

### 3. Total Versus Fast Monsoon Precipitation Response to Aerosol Forcing

What is the monsoon rainfall response to anthropogenic aerosols and how much can it be explained by the fast adjustment? Figures 1a and 1b show the summertime precipitation change to aerosol forcing for (a) total and (b) fast responses, using MMMs of CGCMs and AGCMs, respectively. The total response (Figure 1a) displays a strong drying pattern, consistent with Li et al. (2015) using a larger ensemble set of 35 models. This drying pattern in the coupled models is largely reproduced by the AGCMs without the SST feedbacks (Figure 1b), particularly over eastern China and northern India. On the other hand, between  $0^\circ$  and  $20^\circ\text{N}$  over the oceanic regions as well as southern India, the fast response (Figure 1b) shows a wetting trend that opposes the total response (Figure 1a). The similarity between Figures 1a and 1b to the north of  $20^\circ\text{N}$  indicates that the fast adjustments dominate the monsoon rainfall response over the majority of the land regions, with an even stronger drying than the total response over eastern China.

The overall drying in the total response and the meridional land-ocean dipole structure in the fast response are largely robust using a larger set of available models (Figure S1). Separating the models with and without a fully interactive aerosol scheme further shows that the aerosol indirect effects (aerosol-cloud interactions) dominate both the total and fast responses, particularly in the fast response which indicates almost no signal over land in models without fully interactive aerosols (Figure S1). Among the five common models, the one model with semiinteractive aerosols (IPSL-CM5A-LR) shows much weaker responses compared to the other models with fully interactive aerosols (Figures S2 and S3).

It should be noted that the total and fast responses are not precisely comparable due to the differences of both model setting and aerosol forcing. The fast response is quantified using idealized AGCMs without the coupling to the ocean, which differs from the fully coupled model used in the total response. Furthermore, the aerosol forcing corresponding to these two responses are slightly different since the CGCMs are transient runs in which the aerosol forcing changes with time, whereas the AGCMs have fixed aerosol forcing. As shown in Figures 1c and 1d using three models with available data, the response in aerosol optical depth (AOD) at 550 nm corresponding to the total and fast rainfall responses are almost identical in both magnitude and spatial distribution over Asia, lending support to the comparison between the aerosol-induced rainfall changes. However, it should be noted that the differences between the AOD patterns, particularly over Europe, may cause remote influences on the Asian monsoon (Bollasina et al., 2014).

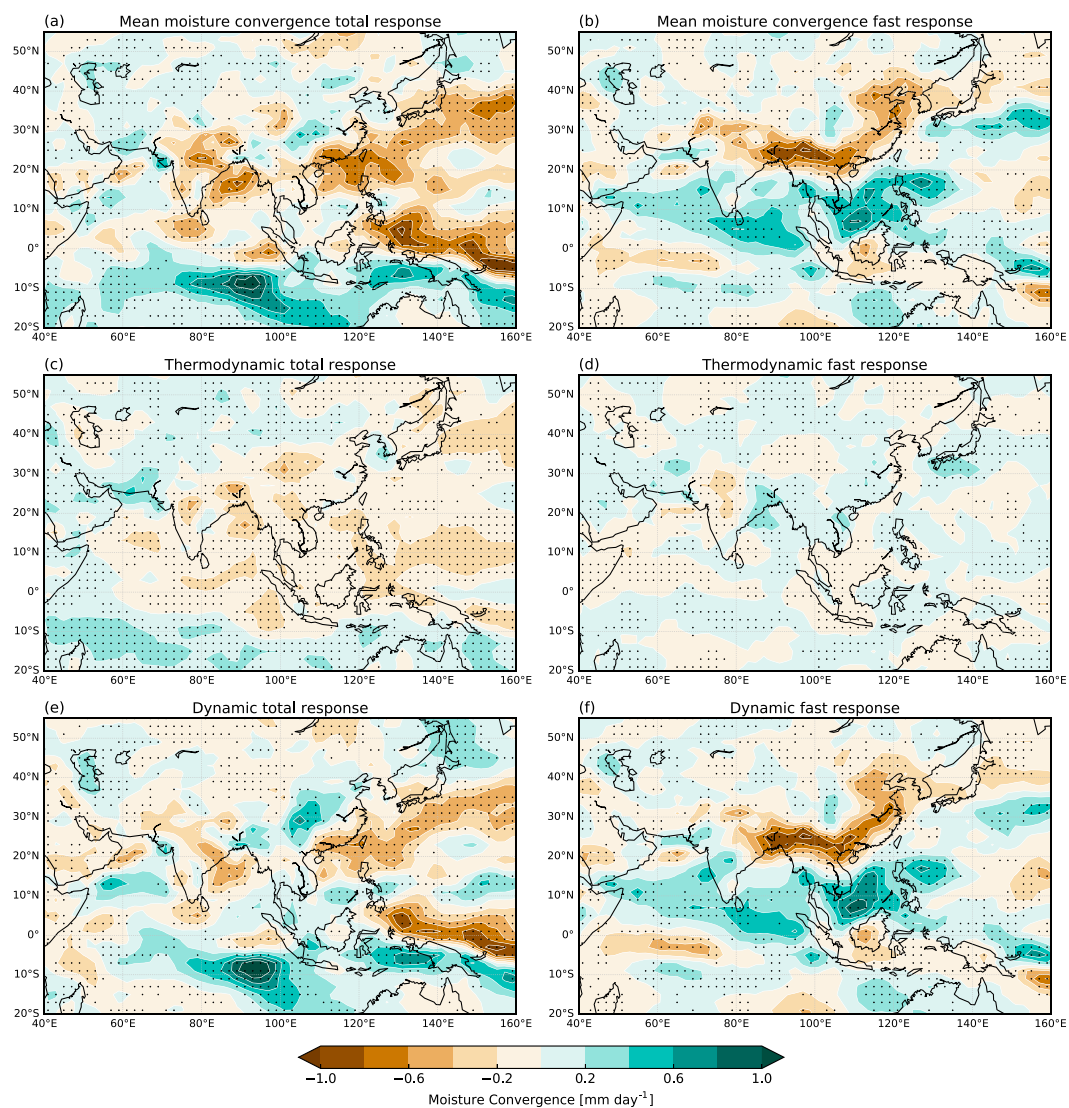


**Figure 2.** The moisture budget response separating into thermodynamic (moisture) and dynamic (circulation) contributions. (a, c, and e) Total response in CGCMs and (b, d, and f) fast response in AGCMs of the mean moisture convergence (Figures 2a and 2b) ( $\delta\overline{MC}$ ), the thermodynamic component ( $\delta\overline{TH}$ ) (Figures 2c and 2d), and the dynamic component ( $\delta\overline{DY}$ ) (Figures 2e and 2f). Stippling denotes four out of five models agree on the sign of change. Units are  $\text{mm d}^{-1}$ .

#### 4. Identifying Mechanisms of Aerosol-Induced Monsoon Changes on Different Time Scales

Monsoon rainfall is controlled by both moisture supply (thermodynamics) and atmospheric circulation (dynamics). What are their relative roles in shaping the responses in Figures 1a and 1b? We use the atmospheric moisture budget analysis to quantify the thermodynamic and dynamic mechanisms contributing to the rainfall changes, as illustrated in Figure 2. Changes in the column-integrated mean moisture convergence ( $\delta\overline{MC}$ , Figures 2a and 2b) balances well with the net surface water budget, precipitation minus evaporation ( $\delta(\overline{P} - \overline{E})$ , Figure S4), in both the CGCMs and AGCMs, confirming that the transient eddies play a minor role over the monsoon region (Figure S5). Consistent with Li et al. (2015) using a slightly larger ensemble set of nine models, the total response of  $\delta\overline{MC}$  (Figure 2a) is a combination of thermodynamic ( $\delta\overline{TH}$ , Figure 2c) and dynamic ( $\delta\overline{DY}$ , Figure 2e) effects, resulting in a strong decrease of moisture convergence. However, for the fast response, the thermodynamic component ( $\delta\overline{TH}$ , Figure 2d) contributes very little due to the limited moisture

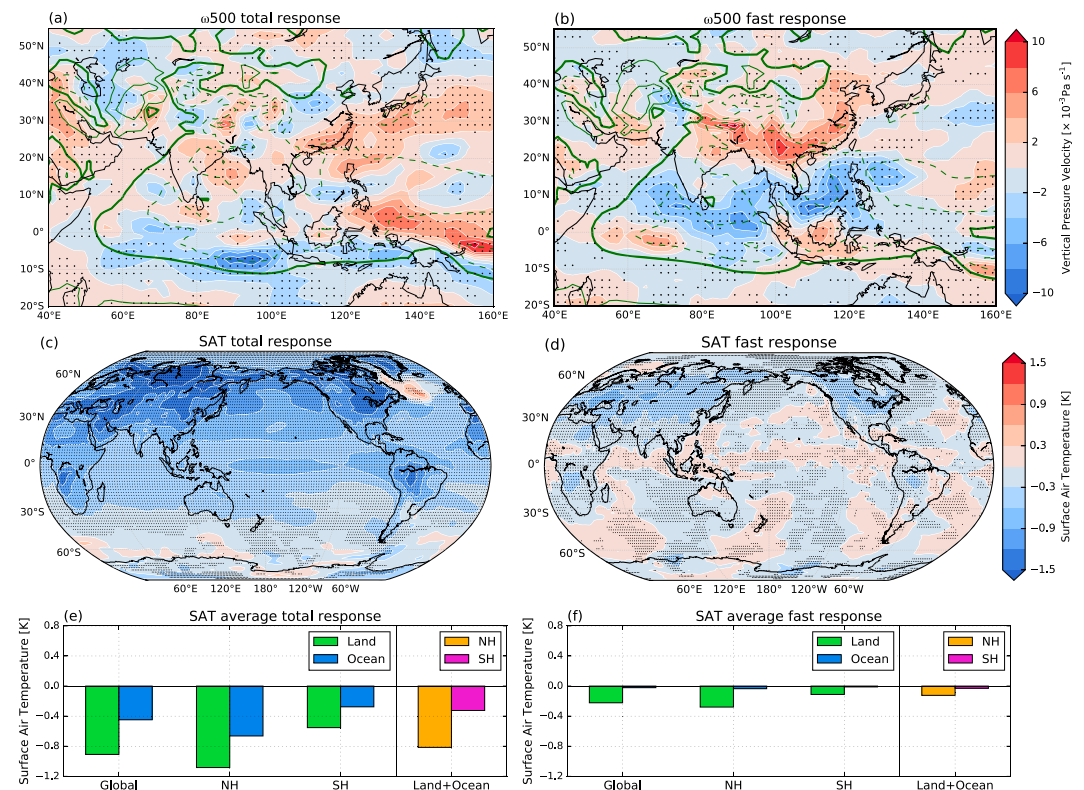


**Figure 3.** Vertical motion response and the contribution of the meridional temperature gradient. (a, c) Total and (b, d) fast responses of 500 hPa vertical pressure velocity ( $\omega$ ) (Figures 3a and 3b) and surface air temperature (Figures 3c and 3d). In Figures 3a and 3b, contours show climatological values of 1861–1885 for Figure 3a and the control simulation climatology for Figure 3b. Solid (dashed) contours show positive (negative) values, indicating sinking (rising) motion. Contour intervals are  $0.04 \text{ Pa s}^{-1}$ . The thick solid contour denotes 0. Stippling denotes four out of five models agree on the sign of change. (e, f) Area average of (green bar) land-only and (blue bar) ocean-only surface air temperature response for global, Northern Hemisphere, and Southern Hemisphere; the overall Northern and Southern Hemisphere averages are shown in orange and magenta, respectively. Units are  $10^{-3} \text{ Pa s}^{-1}$  for Figures 3a and 3b and K for Figures 3c–3f.

supply from the fixed-SST setting; and the dynamic component ( $\overline{\delta DY}$ , Figure 2f) dominates the strong reduction of the mean moisture convergence, particularly over land to the north of  $20^\circ\text{N}$ .

The dynamical changes for the total and fast responses are confirmed using the 500 hPa vertical pressure velocity ( $\omega$ ) in Figures 3a and 3b. The total response (Figure 3a) shows moderate anomalous sinking motion over most of India and southern China. Between  $0^\circ$  and  $20^\circ\text{N}$ , the response is relatively weak and inhomogeneous with low model agreement, but there is strong anomalous rising motion over the Indian Ocean south of the equator. For the fast response (Figure 3b), unlike the weak response in Ganguly et al. (2012b) and the slight enhancement in Kim et al. (2016), the vertical motion change shows a distinct meridional dipole structure with high model agreement: strong sinking anomalies over the land monsoon regions from northern India to eastern China, and strong rising anomalies to the south over the adjacent oceans as well as southern India. The difference with previous studies as well as within the model ensemble (Figure S3) suggests that the results may be model dependent. This meridional pattern is well reproduced in  $\overline{\delta DY}$  (Figure 2f) and  $\overline{\delta MC}$  (Figure 2b).

The difference between Figures 3a and 3b, particularly the absence of the strong rising anomaly over the oceans at  $0^\circ$ – $20^\circ\text{N}$  in the total response, suggests that the slow response due to SST change may play an important role in shaping the monsoon circulation response over the oceanic regions. Previous studies have addressed the roles of land sea thermal contrasts and SST gradients in determining the aerosol-induced circulation changes (Bollasina et al., 2011; Chung & Ramanathan, 2006; Richardson et al., 2016). Here we show the surface air temperature changes in the total and fast responses in Figures 3c and 3d, respectively, and

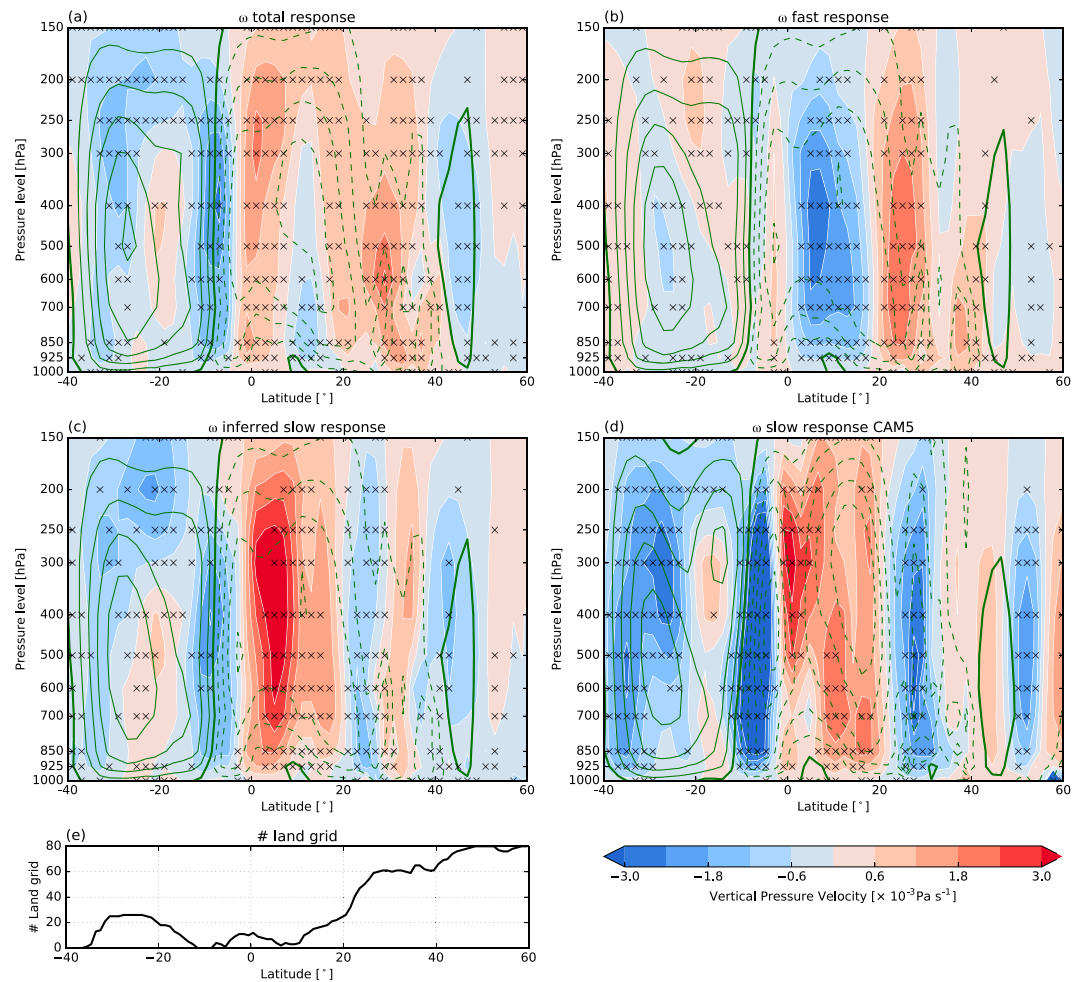


**Figure 4.** Monsoon region atmospheric overturning circulation response. The 60°E to 140°E averaged vertical pressure velocity ( $\omega$ ) of (a) total response in the five CMIP5 CGCMs; (b) fast response in the five AGCMs; (c) the difference between Figures 4a and 4b, approximating the slow response; and (d) slow response in CAM5. Contours show climatological values of 1861–1885 for Figure 4a and the control simulation climatology for Figures 4b–4d. Solid (dashed) contours denote positive (negative) values, indicating sinking (rising) motion. Contour intervals are  $0.009 \text{ Pa s}^{-1}$ . The thick solid contour denotes 0. (e) Total number of land grid points for each latitude (using  $1^\circ \times 1^\circ$  resolution) from 60°E to 140°E. Stippling indicates four out of five models agree on the sign of change for Figures 4a–4c and statistically significant at 5% significance level using two-tailed z test for Figure 4d. Units are  $10^{-3} \text{ Pa s}^{-1}$  for Figures 4a–4d.

area-averaged values in Figures 3e and 3f. While the land (green bars in Figures 3e and 3f) cools off more than the ocean (blue bars in Figures 3e and 3f) in both cases, aerosols also induce a strong meridional temperature gradient with a much cooler Northern Hemisphere in the total response (Figures 3c and 3e), consistent with the stronger aerosol masking effect on global warming shown in Lau and Kim (2017). In the fast response, on the other hand, the temperature change is confined to the continental regions with little change over ocean (Figures 3d and 3f). The meridional temperature gradient in the total response and the land-ocean temperature contrasts in both the total and fast responses are much weaker in the models without fully interactive aerosols (Figure S6), explaining the weaker rainfall responses (Figure S1). The moist static energy (MSE, defined as  $MSE = c_p T + L_v q + gZ$ , where  $c_p$  is the specific heat of air at constant pressure,  $T$  is air temperature,  $L_v$  is the latent heat of vaporization,  $q$  is specific humidity,  $g$  is gravity, and  $Z$  is the geopotential height) response at 925 hPa, which incorporates the effects of both temperature and moisture, shows the large-scale meridional gradient in the total response is largely dominated by the temperature contribution while moisture also contributes over the Indian Ocean (Figure S7).

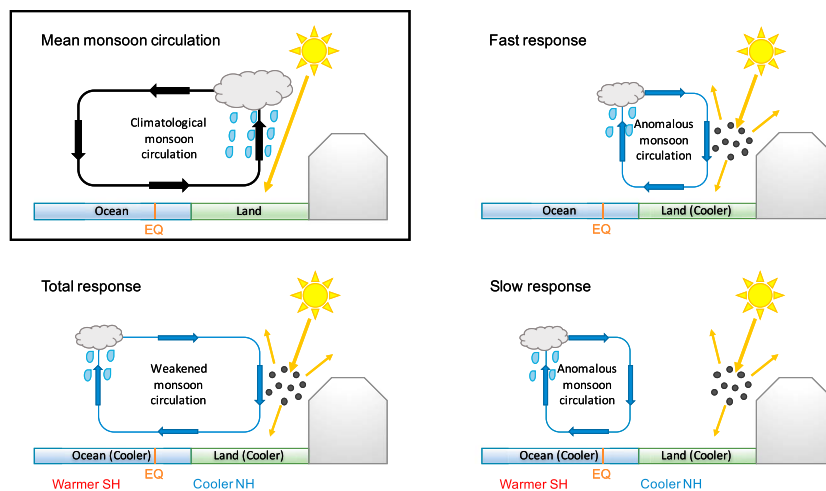


**Figure 5.** Total, fast, and slow monsoon circulation responses to anthropogenic aerosols. On a shorter time scale, aerosols cause a rapid cooling of the local land surface, which induces anomalous sinking motion over land and anomalous rising motion over the adjacent oceans (fast response). On a longer time scale, aerosols cause a decrease in SSTs, as well as a meridional temperature gradient with a stronger cooling in the Northern Hemisphere, resulting in anomalous sinking (rising) motion north (south) of the equator (slow response). The combination of the fast adjustments and SST feedbacks leads to an overall reduction of the local overturning circulation (total response).

The meridional temperature gradient associated with SST feedbacks, coupled with the stronger land cooling, induce significant changes in the local atmospheric overturning circulation. Figure 4 shows the  $60^{\circ}\text{E}$  to  $140^{\circ}\text{E}$  averaged vertical motion change for the total (Figure 4a) and fast (Figure 4b) responses. The climatological rising motion (dashed contours) spans a wide latitude band from  $10^{\circ}\text{S}$  to  $40^{\circ}\text{N}$ , representing an expanded cross-equatorial overturning circulation during the summer monsoon months and the seasonal migration of the Intertropical Convergence Zone (Schneider et al., 2014). The climatological sinking branch (solid contours) is located to the south of  $10^{\circ}\text{S}$ . The AGCMs reproduce well the regional overturning circulation (contours in Figure 4b). The aerosol-induced total response (shading in Figure 4a) features an overall reduction of the climatological circulation with anomalous sinking motion over most of the climatological convection region and anomalous rising motion south of the equator, consistent with previous studies (Bollasina et al., 2011; Li et al., 2015). However, the anomalous sinking motion is confined to the north of  $20^{\circ}\text{N}$  in the fast response (shading in Figure 4b), where the major land mass is located (illustrated by the number of land grid points in Figure 4e). There is strong anomalous rising motion between  $0^{\circ}$  and  $20^{\circ}\text{N}$  over the oceanic regions. The difference between Figures 4a and 4b (Figure 4c, assuming linearity, approximates the “slow response”) shows strong anomalous sinking motion over  $0^{\circ}$ – $20^{\circ}\text{N}$  and anomalous rising motion south of the equator. The slow response due to aerosol-induced SST anomaly in CAM5 (Figure 4d) shows very similar patterns to that in Figure 4c. The consistency between Figures 4c and 4d confirms that the anomalous overturning circulation near the equator is predominantly caused by the slow response due to SST feedbacks.

How does anthropogenic aerosol forcing affect the Asian monsoon circulation? We summarize the different physical pathways in Figure 5. On a shorter time scale without the mediation of SSTs, the addition of anthropogenic aerosols in the atmosphere causes a rapid cooling of the local land surface, which induces anomalous sinking motion over land and anomalous rising motion over the adjacent oceans (fast response). On a longer time scale, aerosol forcing further causes a decrease in SSTs, while also inducing a meridional temperature gradient with a stronger cooling in the Northern Hemisphere due to asymmetry in aerosol emissions between the two hemispheres. Based on the weak temperature gradient approximation, horizontal temperature gradients are small in the tropical atmosphere due to the weak Coriolis effect near the equator (Sobel et al., 2001). As a consequence, an anomalous cross-equatorial upper tropospheric flow occurs to offset the hemispheric temperature and energy imbalance, resulting in anomalous sinking (rising) motion north (south) of the equator (slow response). The combination of the fast adjustments and SST feedbacks, involving competing effects at  $0^{\circ}$ – $20^{\circ}\text{N}$ , causes an overall reduction of the local overturning circulation (total response).

## 5. Summary

Using multiple CGCMs and idealized AGCM experiments, we have identified the physical mechanisms of the total and fast monsoon responses to aerosol forcing. The single-forcing model simulations and the AGCM approach, although highly idealized, provide an effective way to separate the physical processes driving the aerosol-induced monsoon responses on different time scales, essential for furthering the mechanistic understanding and reducing the uncertainties related to aerosol-forced changes. Our results show that the fast adjustment that occurs before surface temperature adjusts to the forcing largely explains the total reduced rainfall over the major land regions, dominated by changes in atmospheric circulation. However, this rainfall suppression over land is largely absent in models where indirect aerosol interaction with clouds is not included. This is similar to the findings for the total aerosol-induced response in Guo et al. (2015) based on 24 CMIP5 CGCMs, associated with a large increase in the cloud droplet number in models with indirect aerosol effects, thus reducing the precipitation efficiency and increasing atmospheric stability in the lower troposphere (Allen & Sherwood, 2010; Lau & Kim, 2017).

We have proposed possible physical pathways by which aerosols impact the local overturning circulation on different time scales. Unlike GHGs with competing effects in the fast and slow responses which lead to an overall weak circulation response (Li & Ting, 2017; Shaw & Voigt, 2015), both the fast and slow responses to aerosol forcing cause an anomalous overturning circulation, however, centered around different latitudes. Both the land-ocean asymmetry and meridional temperature gradient are key factors in determining the aerosol-induced circulation responses. On the other hand, the possible competing effects of the fast and slow responses at the land-ocean boundary where multiple physical processes are entangled may contribute to a higher level of uncertainty. It is also unclear whether the SST feedbacks are dominated by the overall aerosol-induced cooling, the global meridional temperature gradient, or the regional SST pattern, which will be addressed in a subsequent study through further idealized AGCM experiments.

### Acknowledgments

The authors would like to thank Michela Biasutti and Yochanan Kushnir for helpful discussions, and Haibo Liu for downloading and preprocessing the CMIP5 data used in this study. We thank two anonymous reviewers for their helpful comments. We acknowledge the World Climate Research Programme's Working Group on Coupled Modeling, which is responsible for CMIP, and we thank the climate modeling groups (listed in Table S1 of this paper) for producing and making available their model output. For CMIP the U.S. Department of Energy's Program for Climate Model Diagnosis and Intercomparison provides coordinating support and led development of software infrastructure in partnership with the Global Organization for Earth System Science Portals. The CESM project is supported by the National Science Foundation and the Office of Science (BER) of the U.S. Department of Energy. Computing resources were provided by the Climate Simulation Laboratory at NCAR's Computational and Information Systems Laboratory (CISL), sponsored by the National Science Foundation and other agencies. This work was supported by the National Science Foundation grant AGS16-07348. X. L. was supported by National Aeronautics and Space Administration (NASA) Headquarters under the NASA Earth and Space Science Fellowship Program—grant NNX15AP01H. LDEO contribution 8175.

### References

- Allen, M. R., & Ingram, W. J. (2002). Constraints on future changes in climate and the hydrologic cycle. *Nature*, *419*(6903), 224–232. <https://doi.org/10.1038/nature01092>
- Allen, R. J., & Sherwood, S. C. (2010). Aerosol-cloud semi-direct effect and land-sea temperature contrast in a GCM. *Geophysical Research Letters*, *37*, L07702. <https://doi.org/10.1029/2010GL042759>
- Andrews, T., Forster, P. M., & Gregory, J. M. (2009). A surface energy perspective on climate change. *Journal of Climate*, *22*(10), 2557–2570. <https://doi.org/10.1175/2008JCLI2759.1>
- Bollasina, M. A., Ming, Y., & Ramaswamy, V. (2011). Anthropogenic aerosols and the weakening of the South Asian summer monsoon. *Science*, *334*(6055), 502–505. <https://doi.org/10.1126/science.1204994>
- Bollasina, M. A., Ming, Y., & Ramaswamy, V. (2013). Earlier onset of the Indian monsoon in the late twentieth century: The role of anthropogenic aerosols. *Geophysical Research Letters*, *40*, 3715–3720. <https://doi.org/10.1002/grl.50719>
- Bollasina, M. A., Ming, Y., Ramaswamy, V., Schwarzkopf, M. D., & Naik, V. (2014). Contribution of local and remote anthropogenic aerosols to the twentieth century weakening of the South Asian monsoon. *Geophysical Research Letters*, *41*, 680–687. <https://doi.org/10.1002/2013GL058183>
- Bony, S., Bellon, G., Klocke, D., Sherwood, S., Fermein, S., & Denvil, S. (2013). Robust direct effect of carbon dioxide on tropical circulation and regional precipitation. *Nature Geoscience*, *6*(6), 447–451. <https://doi.org/10.1038/NNGEO1799>
- Boucher, O., Randall, D., Artaxo, P., Bretherton, C., Feingold, G., Forster, P., ... Zhang, X. (2013). Clouds and aerosols. In T. Stocker, et al. (Eds.), *Climate change 2013: The physical science basis. Contribution of Working Group I to the Fifth Assessment Report of the Intergovernmental Panel on Climate Change* (pp. 571–657). Cambridge, United Kingdom and New York: Cambridge University Press.
- Chung, C. E., & Ramanathan, V. (2006). Weakening of North Indian SST gradients and the monsoon rainfall in India and the Sahel. *Journal of Climate*, *19*(10), 2036–2045. <https://doi.org/10.1175/JCLI3820.1>
- Ganguly, D., Rasch, P. J., Wang, H., & Yoon, J.-H. (2012a). Climate response of the South Asian monsoon system to anthropogenic aerosols. *Journal of Geophysical Research*, *117*, D13209. <https://doi.org/10.1029/2012JD017508>
- Ganguly, D., Rasch, P. J., Wang, H., & Yoon, J.-H. (2012b). Fast and slow responses of the South Asian monsoon system to anthropogenic aerosols. *Geophysical Research Letters*, *39*, L18804. <https://doi.org/10.1029/2012GL053043>
- GBD MAPS Working Group (2016). Burden of disease attributable to coal-burning and other major sources of air pollution in china (Tech. Rep. Special Report 20). Boston, MA: Health Effects Institute.
- Gong, D.-Y., Ho, C.-H., Chen, D., Qian, Y., Choi, Y.-S., & Kim, J. (2007). Weekly cycle of aerosol-meteorology interaction over China. *Journal of Geophysical Research*, *112*, D22202. <https://doi.org/10.1029/2007JD008888>
- Guo, L., Highwood, E. J., Shaffrey, L. C., & Turner, A. G. (2013). The effect of regional changes in anthropogenic aerosols on rainfall of the East Asian Summer Monsoon. *Atmospheric Chemistry and Physics*, *13*(3), 1521–1534. <https://doi.org/10.5194/acp-13-1521-2013>
- Guo, L., Turner, A. G., & Highwood, E. J. (2015). Impacts of 20th century aerosol emissions on the South Asian monsoon in the CMIP5 models. *Atmospheric Chemistry and Physics*, *15*(11), 6367–6378. <https://doi.org/10.5194/acp-15-6367-2015>
- Hong, J., & Kim, J. (2011). Impact of the Asian monsoon climate on ecosystem carbon and water exchanges: A wavelet analysis and its ecosystem modeling implications. *Global Change Biology*, *17*(5), 1900–1916. <https://doi.org/10.1111/j.1365-2486.2010.02337.x>
- Hsieh, W.-C., Collins, W. D., Liu, Y., Chiang, J. C. H., Shie, C.-L., Caldeira, K., & Cao, L. (2013). Climate response due to carbonaceous aerosols and aerosol-induced SST effects in NCAR community atmospheric model CAM3.5. *Atmospheric Chemistry and Physics*, *13*(15), 7489–7510. <https://doi.org/10.5194/acp-13-7489-2013>

- Hwang, Y.-T., Frierson, D. M. W., & Kang, S. M. (2013). Anthropogenic sulfate aerosol and the southward shift of tropical precipitation in the late 20th century. *Geophysical Research Letters*, *40*, 2845–2850. <https://doi.org/10.1002/grl.50502>
- Jiang, Y., Liu, X., Yang, X.-Q., & Wang, M. (2013). A numerical study of the effect of different aerosol types on East Asian summer clouds and precipitation. *Atmospheric Environment*, *70*, 51–63. <https://doi.org/10.1016/j.atmosenv.2012.12.039>
- Kim, M. J., Yeh, S.-W., & Park, R. J. (2016). Effects of sulfate aerosol forcing on East Asian summer monsoon for 1985–2010. *Geophysical Research Letters*, *43*, 1364–1372. <https://doi.org/10.1002/2015GL067124>
- Kumar, K. K., Rajagopalan, B., Hoerling, M., Bates, G., & Cane, M. (2006). Unraveling the mystery of Indian monsoon failure during El Niño. *Science*, *314*(5796), 115–119. <https://doi.org/10.1126/science.1131152>
- Lau, W. K.-M., & Kim, K.-M. (2017). Competing influences of greenhouse warming and aerosols on Asian summer monsoon circulation and rainfall. *Asia-Pacific, Journal of the Atmospheric Sciences*, *53*(2), 181–194. <https://doi.org/10.1007/s13143-017-0033-4>
- Lau, K.-M., Kim, M.-K., & Kim, K.-M. (2006). Asian summer monsoon anomalies induced by aerosol direct forcing: The role of the Tibetan Plateau. *Climate Dynamics*, *26*(7–8), 855–864. <https://doi.org/10.1007/s00382-006-0114-z>
- Levy, H., Horowitz, L. W., Schwarzkopf, M. D., Ming, Y., Golaz, J.-C., Naik, V., & Ramaswamy, V. (2013). The roles of aerosol direct and indirect effects in past and future climate change. *Journal of Geophysical Research: Atmospheres*, *118*, 4521–4532. <https://doi.org/10.1002/jgrd.50192>
- Li, Z., Lau, W. K.-M., Ramanathan, V., Wu, G., Ding, Y., Manoj, M. G., ... Brasseur, G. P. (2016). Aerosol and monsoon climate interactions over Asia. *Reviews of Geophysics*, *54*, 866–929. <https://doi.org/10.1002/2015RG000500>
- Li, X., & Ting, M. (2015). Recent and future changes in the Asian monsoon-ENSO relationship: Natural or forced? *Geophysical Research Letters*, *42*, 3502–3512. <https://doi.org/10.1002/2015GL063557>
- Li, X., & Ting, M. (2017). Understanding the Asian summer monsoon response to greenhouse warming: The relative roles of direct radiative forcing and sea surface temperature change. *Climate Dynamics*, *49*(7–8), 2863–2880. <https://doi.org/10.1007/s00382-016-3470-3>
- Li, X., Ting, M., Li, C., & Henderson, N. (2015). Mechanisms of Asian summer monsoon changes in response to anthropogenic forcing in CMIP5 models. *Journal of Climate*, *28*(10), 4107–4125. <https://doi.org/10.1175/JCLI-D-14-00559.1>
- Lin, H., & Wu, Z. (2012). Indian summer monsoon influence on the climate in the North Atlantic–European region. *Climate Dynamics*, *39*(1–2), 303–311. <https://doi.org/10.1007/s00382-011-1286-8>
- Ming, Y., Ramaswamy, V., & Persad, G. (2010). Two opposing effects of absorbing aerosols on global-mean precipitation. *Geophysical Research Letters*, *37*, L13701. <https://doi.org/10.1029/2010GL042895>
- Neale, R. B., Chen, C.-C., Gettelman, A., Lauritzen, P. H., Park, S., Williamson, D. L., ... Taylor, M. A. (2012). Description of the NCAR Community Atmosphere Model (CAM 5.0) (Tech. Rep. NCAR/TN-486+STR). Boulder, CO: National Center for Atmospheric Research (NCAR).
- Piao, S., Ciais, S., Huang, Y., Shen, Z., Peng, S., Li, J., ... Fang, J. (2010). The impacts of climate change on water resources and agriculture in China. *Nature*, *467*(7311), 43–51. <https://doi.org/10.1038/nature09364>
- Ramanathan, V., Chung, C., Kim, D., Bettge, T., Buja, L., Kiehl, J. T., ... Wild, M. (2005). Atmospheric brown clouds: Impacts on South Asian climate and hydrological cycle. *Proceedings of the National Academy of Sciences of the United States of America*, *102*(15), 5326–5333. <https://doi.org/10.1073/pnas.0500656102>
- Rayner, N. A., Parker, D. E., Horton, E. B., Folland, C. K., Alexander, L. V., Rowell, D. P., ... Kaplan, A. (2003). Global analyses of sea surface temperature, sea ice, and night marine air temperature since the late nineteenth century. *Journal of Geophysical Research*, *108*, D144407. <https://doi.org/10.1029/2002JD002670>
- Richardson, T. B., Forster, P. M., Andrews, T., & Parker, D. J. (2016). Understanding the rapid precipitation response to CO<sub>2</sub> and aerosol forcing on a regional scale. *Journal of Climate*, *29*(2), 583–594. <https://doi.org/10.1175/JCLI-D-15-0174.1>
- Rodwell, M. J., & Hoskins, B. J. (1996). Monsoons and the dynamics of deserts. *Quarterly Journal of the Royal Meteorological Society*, *122*(534), 1385–1404. <https://doi.org/10.1002/qj.49712253408>
- Schneider, T., Bischoff, T., & Haug, G. H. (2014). Migrations and dynamics of the intertropical convergence zone. *Nature*, *513*(7516), 45–53. <https://doi.org/10.1038/nature13636>
- Seager, R., & Henderson, N. (2013). Diagnostic computation of moisture budgets in the ERA-Interim reanalysis with reference to analysis of CMIP-archived atmospheric model data. *Journal of Climate*, *26*(20), 7876–7901. <https://doi.org/10.1175/JCLI-D-13-00018.1>
- Shaw, T. A., & Voigt, A. (2015). Tug of war on summertime circulation between radiative forcing and sea surface warming. *Nature Geoscience*, *8*(7), 560–566. <https://doi.org/10.1038/ngeo2449>
- Singh, D. (2016). South Asian monsoon: Tug of war on rainfall changes. *Nature Climate Change*, *6*(1), 20–22. <https://doi.org/10.1038/nclimate2901>
- Sobel, A. H., Nilsson, J., & Polvani, L. M. (2001). The weak temperature gradient approximation and balanced tropical moisture waves. *Journal of the Atmospheric Sciences*, *58*(23), 3650–3665. [https://doi.org/10.1175/1520-0469\(2001\)058<3650:TWTGAA>2.0.CO;2](https://doi.org/10.1175/1520-0469(2001)058<3650:TWTGAA>2.0.CO;2)
- Taylor, K. E., Stouffer, R. J., & Meehl, G. A. (2012). An overview of CMIP5 and the experiment design. *Bulletin of the American Meteorological Society*, *93*(4), 485–498. <https://doi.org/10.1175/BAMS-D-11-00094.1>
- Turner, A. G., & Annamalai, H. (2012). Climate change and the South Asian summer monsoon. *Nature Climate Change*, *2*(8), 587–595. <https://doi.org/10.1038/nclimate1495>